

## Prediction of forming effects in UD-NCF by macroscopic forming simulation – Capabilities and limitations

Luise Kärger, Siegfried Galkin, Eckart Kunze, Maik Gude and Bastian Schäfer

Luise Kärger. Karlsruhe Institute of Technology (KIT), Institute of Vehicle System Technology (FAST), Karlsruhe, Germany

Corresponding author: [luise.kaerger@kit.edu](mailto:luise.kaerger@kit.edu)

Siegfried Galkin. Karlsruhe Institute of Technology (KIT), Institute of Vehicle System Technology (FAST), Karlsruhe, Germany

Federal Waterways Engineering and Research Institute (BAW), Karlsruhe, Germany

Eckart Kunze. Technical University Dresden, Institute of Lightweight Engineering and Polymer Technology (ILK), Dresden, Germany

Maik Gude. Technical University Dresden, Institute of Lightweight Engineering and Polymer Technology (ILK), Dresden, Germany

Bastian Schäfer. Karlsruhe Institute of Technology (KIT), Institute of Vehicle System Technology (FAST), Karlsruhe, Germany

**Abstract.** Unidirectional non-crimp fabrics (UD-NCF) provide the highest lightweight potential among dry textile materials. Compared to multiaxial NCF, the fabric layers in UD-NCF enable a more targeted tailoring. Compared to woven fabrics, the fibres of UD-NCF are straight without weakening undulations. However, the formability of UD-NCF is more challenging compared to woven fabrics. The yarns are bonded by a stitching and the deformation behaviour highly depends on this stitching and on the slippage between the stitching and the fibre yarns. Moreover, distinct local draping effects occur, like gapping and fibre waviness, which can have a considerable impact on the mechanical performance. Such local effects are particularly challenging or even impossible to be predicted by macroscopic forming simulation. The present work applies a previously published macroscopic UD-NCF modelling approach to perform numerical forming analyses and evaluate the prediction accuracy of forming effects. In addition to fibre orientations and shear angles, as investigated in previous work, the present work also provides indication for fibre area ratios, gapping, transverse compaction and fibre waviness. Moreover, the prediction accuracy is validated by comparison with experimental tests, where full-field strains of inner plies are captured by prior application of dots onto the fibre yarns, by measuring them via radiography and applying a photogrammetry software. The modelling approach provides good prediction accuracy for fibre orientations, shear strains and fibre area ratio. Conversely, normal fibre strains, indicating fibre waviness, and transverse strains, indicating gapping, show some deviations due to the multiscale nature of UD-NCF that cannot be captured entirely on macroscopic scale.

**Keywords.** Non-orthogonal Material Modelling, Non-crimp Fabrics, Draping Effects, Gapping, Waviness

## 1 Introduction

Non-crimp fabrics (NCF) provide an exceptionally high lightweight potential due to their straight fibres, compared to undulated fibres in woven fabrics. Among NCFs, unidirectional (UD) NCFs enable a more targeted tailoring than biaxial NCFs. However, their formability is much more challenging in comparison to bidirectional fabrics, and draping effects like shearing, waviness or fibre gapping have a significant impact on the structural performance [1]-[3]. The experimental determination of those effects especially in inner layers of a multi-ply component is challenging and requires dedicated measurement methods [4]. Draping simulations can more easily provide the necessary local information, however need to be suitable and reliable. Mallach et al. [5] conducted optical robot-based measurements of preforming tests to determine shear angles and fibre orientations on the entire surface. They compared the measurements to a macroscopic approach with built-in methods in PAM-FORM and achieved a good prediction of the preform contour and critical regions regarding wrinkling. However, mesoscopic effects like transverse compression, fibre sliding and yarn buckling were not considered in their approach, which led to highly overestimated shear angles as well as large deviations of the fibre orientation.

Macroscopic approaches can predict component forming results efficiently for complexly curved geometries with case-specific process conditions. Due to their better formability, woven fabrics have so far been the focus of research on macroscopic forming models [6]-[8]. In contrast, forming of Biaxial-NCF [9], [10] or even UD-NCF [5], [11]-[14] has been investigated much less and mostly based on mesoscopic approaches, which are not suitable for component forming simulations. In contrast to mesoscopic modelling, macroscopic approaches are not able to discretely predict local forming effects. Nevertheless, they need to capture the relevant forming mechanisms occurring on meso-scale in a homogenized way and consequently indicate areas with a high likelihood of local effects like waviness, transverse compaction or gapping [15]. This desired capability of macroscopic forming simulation of UD-NCF has not yet been addressed in the literature. According to the current state of research and to the authors' knowledge, the modelling approach proposed by Schirmaier et al. [11] is the most promising macroscopic UD-NCF model available to date. It considers both large-strain deformation and non-linear constitutive behaviour. To account for the permanent deformation caused by irreversible slip between fibre yarns, stitching and glass fibres, an elastic-plastic material model is chosen to capture the experimentally observed non-linearity of the macroscopic stress-strain relation [11], [13], [16].

In previous work, the prediction accuracy of Schirmaier's model was shown only by qualitative comparison to component forming results [11], without full-field quantitative validation nor evaluation of specific forming effects. Therefore, the model is applied in the present work to forming of an L-shaped geometry in order to quantitatively evaluate the prediction quality regarding global and local forming effects. The results are compared to radiography measurements of internal plies based on the method presented in Kunze et al. [4]. The measurement method allows for the determination of the local deformation, which gives a direct measure not only for fibre orientations, but also for forming effects like gapping, waviness and transverse compression, enabling an estimation, e.g., of the local fibre volume content [17]. Subsequently, the suitability of the macroscopic approach to predict these local effects is evaluated.

## 2 Macroscopic forming simulation of UD-NCF

The yarns of non-crimp fabrics (NCF) are bonded together by a stitching pattern and glass fibres for handleability. This is in contrast to woven fabrics, which are intrinsically cohesive due to the interwoven fibre yarns. Consequently, the inherent deformation modes of the two types of textiles differ considerably. Woven fabrics deform in pure shear, while shear in UD-NCF can be superimposed by substantial transverse strain [12], [16]. This superposed membrane behaviour needs to be captured by macroscopic material models in a suitable way. In previous work [11], extensive off-axis-tension (OAT) tests have been performed to analyse the multiaxial deformations at meso and macro scale, and to develop a macroscopic material model for the membrane behaviour. This macroscopic model is shortly presented in the following section and is subsequently applied to investigate the prediction of forming effects.

### 2.1 Non-orthogonal elastic-plastic material model

Macroscopic modelling approaches account for material inhomogeneities in a homogenized way to allow an efficient description of the most relevant deformation mechanisms. The utilized membrane modelling [11] is able to capture large shear strains  $\gamma_{12}$  superimposed with large non-orthogonal transverse tensile strains  $\varepsilon_2$  and orthogonal compressive strains  $\varepsilon_{\perp}$ , cf. Fig. 1(a). Tensile strains  $\varepsilon_2$  (elongated stitching) and compressive strains  $\varepsilon_{\perp}$  (transverse compaction) may occur simultaneously, particularly for large shear strains  $\gamma_{12}$ . The macroscopic approach, however, does not allow for a discrete modelling of the slipping between carbon fibre tows, glass fibres and stitching. Therefore, gapping can only be indicated by large tensile strain  $\varepsilon_2$  at moderate shear strain  $\gamma_{12}$  or, more suitably, by large transverse tensile strains  $\varepsilon_{\perp}$ .

Modelling large non-orthogonal and non-linear deformation of the stitching requires suitable strain and stress measures. For UD-NCF, Schirmaier et al. [11] proposed a formulation for appropriate linear strain and corresponding nominal stress measures. Line segment  $\mathbf{t}_{10}$  represents the material's first principal direction, oriented in fibre direction. Line segment  $\mathbf{t}_{20}$  corresponds to the direction of the stitching, cf. Fig. 1(b). After deformation, the linear but non-orthogonal strain components  $\varepsilon_1$  of the fibres and  $\varepsilon_2$  of the stitching are defined by:

$$\varepsilon_i = \frac{|\mathbf{t}_i|}{|\mathbf{t}_i^0|} - 1 = \sqrt{\sum_j F_{ji}^2} - 1, \quad j = 1,2 \quad (1)$$

where the line segments  $\mathbf{t}_i = \mathbf{F} \cdot \mathbf{t}_i^0$  of the current configuration result from the deformation gradient  $\mathbf{F}$ . The shear angle  $\gamma_{12}$  is calculated by:

$$\gamma_{12} = \frac{\pi}{2} - \psi_{12} = \frac{\pi}{2} - \cos^{-1} \left( \frac{\mathbf{t}_1 \cdot \mathbf{t}_2}{|\mathbf{t}_1| |\mathbf{t}_2|} \right) \quad (2)$$

Additionally, the linear perpendicular strain component  $\varepsilon_{\perp}$  is introduced based on the line segment  $\mathbf{t}_{\perp}$  perpendicular to  $\mathbf{t}_1$ :

$$\varepsilon_{\perp} = \frac{|\mathbf{t}_{\perp}|}{|\mathbf{t}_{\perp}^0|} - 1 = \frac{|\mathbf{t}_2| \sin(\psi_{12})}{|\mathbf{t}_2^0|} - 1 = \sqrt{F_{12}^2 + F_{22}^2} \sin(\psi_{12}) - 1 \quad (3)$$

cf. Fig. 1(a) [11].

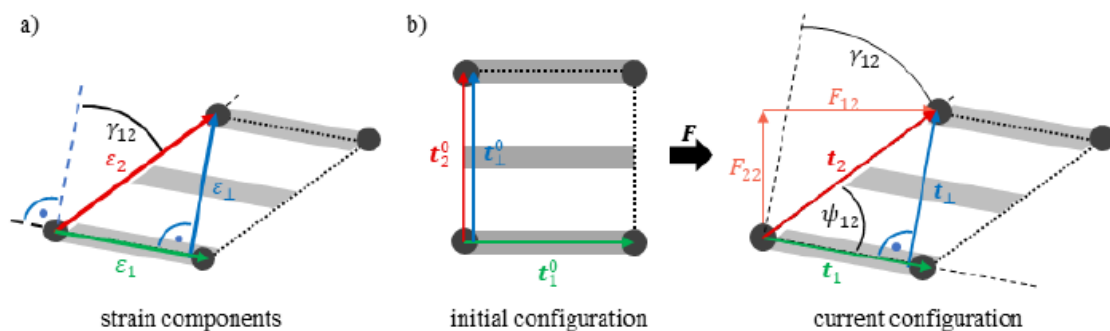


Fig. 1. (a) Transverse strain  $\varepsilon_2$  versus perpendicular strain  $\varepsilon_{\perp}$ ; (b) deformation of line segments  $\mathbf{t}_1$ ,  $\mathbf{t}_2$  and  $\mathbf{t}_{\perp}$ , based on [11], [15]

In the corresponding alternative intermediate configuration, the nominal stress tensor  $\mathbf{P}^*$  can be formulated based on an orthogonal material stiffness matrix by:

$$\underline{P}^* = \begin{pmatrix} P_{11}^* \\ P_{22}^* \\ P_{21}^* \end{pmatrix} = \begin{pmatrix} \frac{E_1}{1 - \nu_{12}\nu_{21}} & \frac{\nu_{21}E_1}{1 - \nu_{12}\nu_{21}} & 0 \\ \frac{\nu_{12}E_2}{1 - \nu_{12}\nu_{21}} & \frac{E_2}{1 - \nu_{12}\nu_{21}} & 0 \\ 0 & 0 & G_{12} \end{pmatrix} \begin{pmatrix} \varepsilon_1 \\ \varepsilon_2 \\ \gamma_{12} \end{pmatrix} \quad (4)$$

accounting for large shear strains  $\gamma_{12}$  and the non-orthogonal linear strains  $\varepsilon_1, \varepsilon_2$ . In this intermediate configuration, the line segments remain in their initial orientation, elongated to the current configuration, based on an alternative decomposition of the deformation gradient  $\mathbf{F}$  described in [11].

To account for elastic-plastic behaviour, the total tensile strain  $\varepsilon_2$  and the total shear angle  $\gamma_{12}$  are composed of elastic as well as hardening plastic parts [11]. A yield condition defines the transition from elastic to plastic domain. Material parameter fitting led to the conclusion, that in case of tensile loading of the stitching, the respective yield surface  $R_{2T}(\varepsilon_{2,p}, \gamma_{12})$  depends on the plastic strain  $\varepsilon_{2,p}$  as well as on the shear angle  $\gamma_{12}$ , while in case of shear loading the yield curve  $R_{12T}(\gamma_{12,p})$  only depends on the plastic shear  $\gamma_{12,p}$ .

Transverse compression can only be transmitted perpendicular to the carbon fibres. This compressive stress  $P_{\perp}$  is modelled via a superimposed nonlinear elastic material law depending on  $\varepsilon_{\perp}$  and  $\gamma_{12}$  to account for the fact that macroscopic wrinkling starts at higher in-plane transverse compression in case of high shear angles [11]. If perpendicular strain  $\varepsilon_{\perp}$  and transverse strain  $\varepsilon_2$  have equal sign, disjunction needs to be ensured. Therefore, the transverse stress  $P_{22}^*$  is set to zero for  $\varepsilon_2 < 0$  and the perpendicular stress  $P_{\perp}$  is set to zero for  $\varepsilon_{\perp} > 0$ . A more detailed description of the non-orthogonal-plastic UD-NCF membrane model is given in [11]. The model parameters for shear and transverse tension have been identified based on experimental off-axis tension (OAT) tests of UD-NCF with three different fibre orientations  $\theta = \{30^\circ, 45^\circ, 60^\circ\}$  [11], [17].

The bending behaviour of UD-NCF is modelled by a hypoelastic approach, initially introduced for thermoplastic UD-tapes [18]. Bending stiffness stays orthogonal in case of large shear deformation and only requires an accurate rotation of the unidirectional carbon fibres (line segment  $\mathbf{t}_1$ ). The behaviour is assumed to be linear elastic and is defined by the bending stiffness in fibre direction  $E_{||}^B$  and negligible stiffness perpendicular  $E_{\perp}^B$  to the fibres.

## 2.2 Forming simulation model

The forming simulation model is implemented in ABAQUS. Since the high membrane stiffness in fibre direction is combined with a very low bending stiffness, the deformation behaviour cannot be captured by conventional shell theories based on Cauchy mechanics. Therefore, membrane and bending behaviour is modelled by superimposed finite membrane and plate elements. The non-orthogonal elastic-plastic material model of the membrane behaviour is implemented in a VUMAT subroutine [11]. For the plate element, a user-defined shell section integration is implemented in a VUGENS subroutine [18]. The interface behaviour between the individual plies as well as between tool and plies is modelled by combined normal and tangential contact, depending on normal pressure, slip-rate and adhesion [18]. The contact model is implemented in a VUINTERACTION subroutine.

## 2.3 Prediction of forming effects

Forming of UD-NCF is largely determined by the low shear and low transverse stiffness that highly depend on the type of stitching and on the slippage between stitching and fibre yarns. The fibre orientation of the current configuration  $\mathbf{t}_1 = \mathbf{F} \cdot \mathbf{t}_1^0$  is computed by the initial fibre orientations  $\mathbf{t}_1^0$  and the deformation gradient  $\mathbf{F}$ . The shear angle  $\gamma_{12}$  results from

Eq. (2). Transverse tensile or compressive deformation leads to gapping between fibre yarns or transverse compaction, respectively. Furthermore, mesoscopic buckling of the fibre yarns may occur due to lateral contraction of the stitching [16]. Assuming a constant fabric weight, the fibre volume content (FVC)

$$\varphi_f = \frac{A}{A_0} \varphi_{f0} \quad (5)$$

depends on the initial FVC  $\varphi_{f0}$  and on the ratio between the initial area  $A_0$  and the deformed area

$$A = \det(\mathbf{F}) A_0 = (F_{11}F_{22} - F_{12}F_{21})A_0 \quad (6)$$

In addition to fibre orientation, shear angle and FVC, the modelling approach provides indication to analyse three further forming effects: gapping, transverse compaction and fibre waviness [15], [17]. Thereby, observations based on extensive OAT tests have shown, that the non-orthogonal tensile strain component  $\varepsilon_2$  (stitching) is not suitable for indicating gapping nor transverse in-plane compressive behaviour. Component forming simulations have shown that the perpendicular strain component  $\varepsilon_{\perp}$  is more suitable for that purpose, to indicate, where gapping corresponds to tensile strains and compaction to compressive strains [11].

Fibre waviness occurs at meso scale and cannot be captured macroscopically. Such undulations typically arise in regions with compressive fibre strain,  $\varepsilon_1 < 0$ , due to fibre buckling. Hence, an assessment of the amplitude to wavelength ratio  $A_{\lambda}/\lambda$  can be deduced from  $\varepsilon_1$ . However, it depends on the compressive stiffness of the fibre yarn, which has not been measured and thus impedes a quantitative evaluation. Nevertheless, a qualitative evaluation of the susceptibility to waviness can be conducted, e.g., for varying process conditions [15].

### 3 Application, results and discussion

#### 3.1 Reference structure and experimental test setup

An L-shaped geometry as shown in Fig. 2a is chosen to analyse the different types of forming effects qualitatively and quantitatively. Due to the multiple curvatures and draft angles, locally varying degrees of forming can be observed. Furthermore, nineteen individually controllable blank holders are installed (Fig. 2b) to manipulate the draping process and to influence the formation of draping effects like waviness, gapping or compaction [4],[15]. In the experimental test programme, two-layer and eight-layer unidirectional (UD) and bidirectional (BD) layups of carbon fibre (CF) UD-NCF (Zoltek PX 35 50 K, 338 g/m<sup>2</sup>) were formed using different blank-holder configurations.

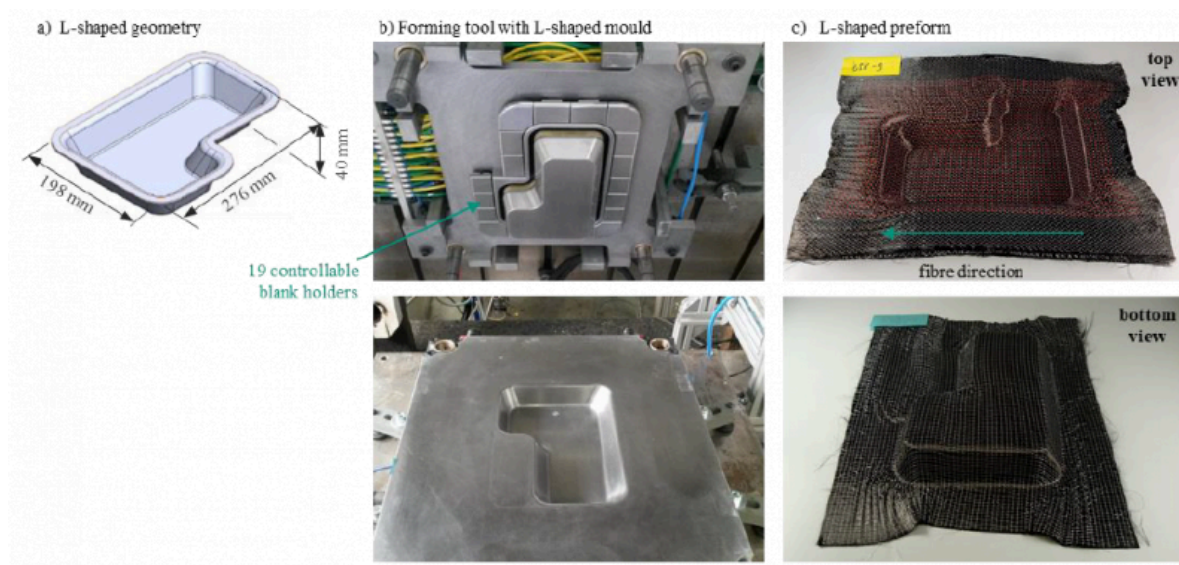


Fig. 2. (a) L-shaped geometry. (b) Forming tool with 19 controllable blank holders and L-shaped negative mould. (c) Top and bottom view of a UD-NCF preform with 8 layers Zoltek PX35 and with a red dot grid printed on top layer [4]

To analyse the resulting fibre orientations and the extent of forming effects in inner layers, a contrast-enhancing ink used in X-rays is printed in a dot pattern on the fibre bundles (Fig. 3a) and is evaluated by radiography images [4]. To analyse outer plies, the method can also be applied with simple coloured points and a photo camera, cf. Fig 2c (top). In this way, the deformation of individual fabric plies can be quantified locally, which gives a direct measure for the fibre orientation as well as for forming effects like gapping and transverse compression, and thus enables an estimation of the local fibre volume content [17]. Based on the measurements, a comparison with forming simulation can be conducted by exporting the coordinates of the acquired 3D points and computing the deformation gradient in relation to the reference state. Thus, a high-resolution quantification of the forming effects becomes feasible for inner plies, cf. Fig. 3.



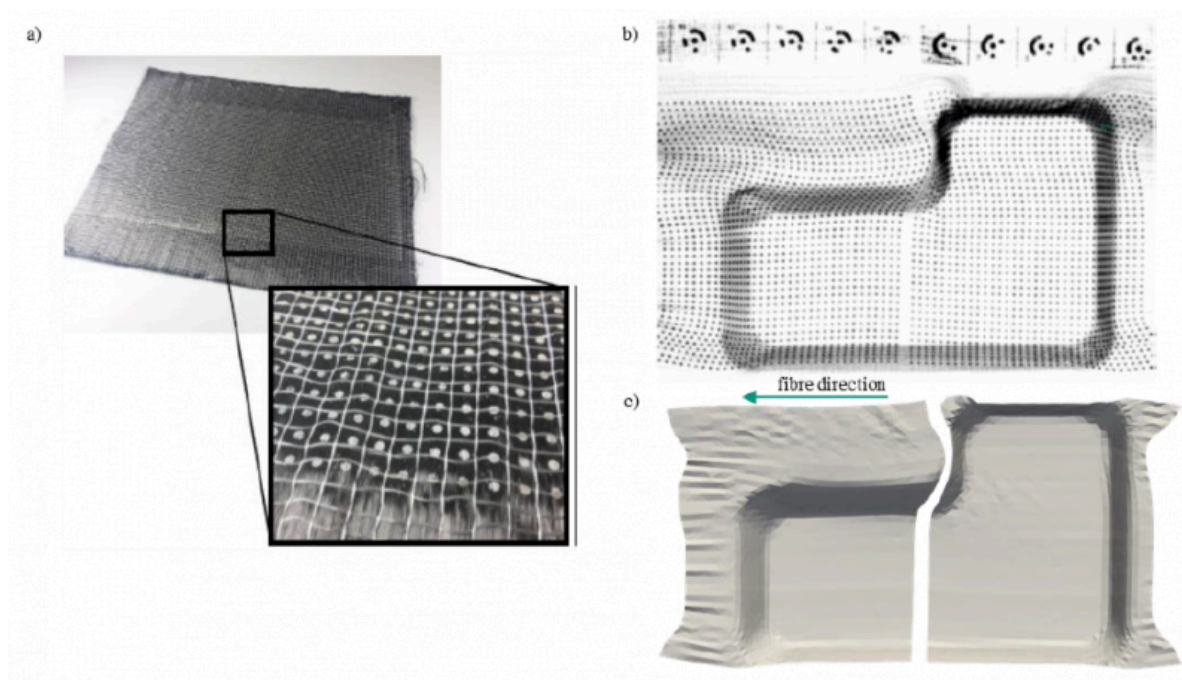


Fig. 3. (a) Silver dot grid on semi-finished NCF. (b) Detected dot grid on a deformed UD-NCF with associated reference markers [4]. (c) Deformed UD-NCF layer, deduced from the radiographic measurements

### 3.2 Comparison of experimental and simulation results

For experimental analysis, the dot grid is applied on the fourth layer (Fig. 3a) and three preforms of identical configuration are evaluated to account for the scattering during forming. A comparison between the three configurations showed a very good agreement with negligible deviations. After forming, the coordinates of the displaced dots and the resulting local deformation gradients are determined. Based on the deformation gradient, local fibre orientations, area changes and strain measures can be evaluated. According to the UD-NCF material model presented in Section 2.1, relevant strain measures are the strain components  $\varepsilon_1$  of the fibres and  $\varepsilon_2$  of the stitching, the perpendicular transverse strain  $\varepsilon_{\perp}$  and the shear angle  $\gamma_{12}$  between the fibre direction and the second material axis. These can be evaluated and compared to simulation results.

For forming simulation, the FE model is built up with superimposed membrane and shell elements as described in Section 2.2. The geometry and the blank holder configurations are defined according to the experimental test setup. To compare experimental and numerical results, they are transferred to a neutral VTK format and to a uniform mesh. The mapping library MpCCI.MapLib from Fraunhofer SCAI [19] is used to map both, the data from the experiments and the data from the simulations, to the uniform mesh.

The comparison between experimental and simulation results is illustrated in Fig. 4 and shows good agreement regarding fibre orientation  $\alpha$  and local area change  $\det(\mathbf{F})$ , with an average deviation of only  $\pm 2^\circ$  in fibre orientation and  $\pm 3\%$  in fibre volume content. Since the thickness of the stack is defined by a constant cavity height, the area change is directly related to the fibre volume content. The largest deviations occur in areas, where the preform recedes after removal from the mould. Similarly, a good agreement of the shear deformation  $\gamma_{12}$  could be observed, with only about  $2^\circ$  mean shear angle deviation.

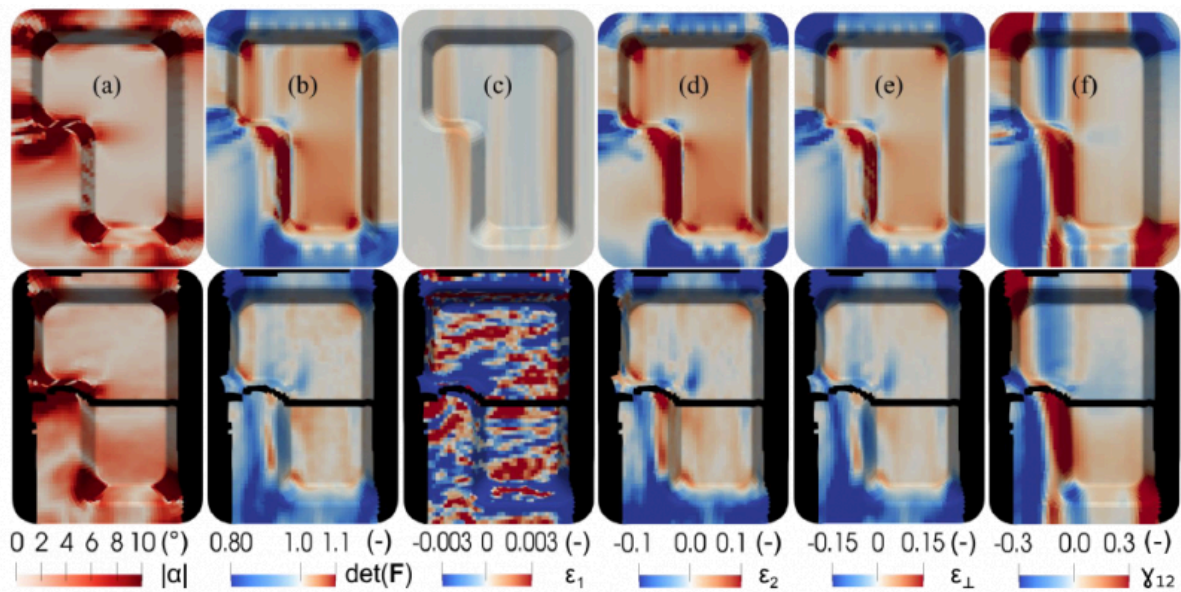


Fig. 4. Comparison between draping simulation (top) and experiment (bottom, black areas without measurement result): (a) deviation from initial fibre orientation, (b) local area ratio, (c) roving elongation, (d) sewing thread elongation, (e) transverse elongation to fibre direction, and (f) shear

The largest deviations occur in the elongation  $\epsilon_1$  in fibre direction and  $\epsilon_{\perp}$  in perpendicular direction, as well as in the elongation  $\epsilon_2$  of the stitching. Due to the assumption of very stiff fibres, the predicted fibre strain in the simulation is very small, whereas the experimental tests show diffuse and wave-like strains, which oscillate between compression and elongation, though at low strain level. In the centre of the geometry a high degree of compression is noticeable and, in this region, a locally clearly visible waviness was found, which indicates the assumption of negative strains in fibre direction as an indicator for the onset of waviness. Similar irregular distributed  $\epsilon_1$  strains have been observed in OAT tests in case of mesoscopic carbon fibre tow buckling due to lateral contraction of the stitching [11]. The largest deviations in the elongation  $\epsilon_2$  of the stitching arise in the area of the inner long side of the L-shaped geometry and in the bottom area, where different running lengths are realized. One possible reason is that the approach presented in Section 2 does not restrict slip between carbon fibre, stitching and glass fibre, and thus, neglects potential load transmission via the glass fibre. This leads to satisfactory results in case of moderate deformations and low blank holder forces [15], but may lead to noticeable deviations, if slip is restricted. For a more accurate prediction of  $\epsilon_1$  the material behaviour in fibre direction needs to be modelled more accurately and advanced modelling approaches are required to capture in-plane fibre bending. Currently, the compressive stiffness in fibre direction is set equal to the constant tensile stiffness and buckling is neglected. Negative  $\epsilon_1$  would then indicate an occurrence of waviness, which in turn leading to non-linear behaviour of the modulus in fibre direction and to in-plane bending of the roving. In-plane bending cannot be captured by approaches based on Cauchy mechanics and requires generalized continuum approaches [20]. Introducing an in-plane fibre bending stiffness, would also enable shear stiffness parallel to the fibre tows (21-shear) to be modelled differently from the macroscopic shear stiffness perpendicular to the fibre tows (12-shear). Experimental tests show that shear deformation primary occurs parallel to the carbon fibres, since in-plane bending stiffness of the carbon fibre tows hinders shear deformation perpendicular to the carbon fibres.

## 4 Conclusions

A macroscopic modelling approach for unidirectional non-crimp fabrics (UD-NCF) is evaluated for its accuracy



in predicting global and local forming effects. The prediction accuracy is validated by experimental tests, where full-field strains are measured by projectional radiography. The modelling approach allows for the prediction of fibre orientations, shear angles and fibre area changes, which all show good agreement with experimental results. Based on its strain measures, the model can also provide indication for fibre waviness, gapping, and transverse compaction. Fibre waviness can be deduced from negative strains in fibre direction, provoking fibre buckling. For a quantitative evaluation, however, the compressive stiffness in fibre direction needs to be known. Furthermore, advanced generalized continuum approaches are required to capture in-plane fibre bending and the resulting reduced stiffness in fibre direction. Consequently, the proposed macroscopic approach can provide only a qualitative, but no quantitative estimation of forming-induced fibre waviness. Transverse compaction and fibre gapping can be deduced from the strain measures transverse and perpendicular to the fibres. Both show some deviations from experimental results particularly in areas, where varying running length in fibre direction need to be formed. To predict gapping and transverse compaction accurately, the multiscale nature of UD-NCF needs to be captured entirely. This includes slip modelling between carbon fibre, stitching and glass fibre, which depends on the deformation state and on boundary conditions. While meso-modelling can capture this behaviour intrinsically, a homogenised formulation for macroscopic modelling remains challenging.

## Acknowledgements

The research documented in this manuscript has been funded by the German Research Foundation (DFG), mainly within the project “Experimental and virtual analysis of draping effects and their impact on the structural mechanical behaviour of fibre composite components” (No. 287275762) and subsequently within the DFG-ANR project “Composite forming simulation for non-crimped fabrics based on generalized continuum approaches” (No. 431354059). The support by the DFG is gratefully acknowledged. The work is also part of the Young Investigator Group (YIG) Tailored Composite Materials for Lightweight Vehicles, thankfully funded by the Vector Stiftung. The authors are also grateful to Fraunhofer SCAI for freely providing MpCCI MapLib.

## Bibliography

- [1] Kunze, E. Galkin, S. Böhm, R. Gude, M. Kärger, L. The impact of draping effects on the stiffness and failure behavior of unidirectional non-crimp fabric fiber reinforced composites. *Materials*, 2020, 13, 2959. DOI 10.3390/ma13132959.
- [2] Kärger, L. Bernath, A. Fritz, F. Galkin, S. Magagnato, D. Oeckerath, A. Schön, A. Henning, F. Development and validation of a CAE chain for UD fibre reinforced composite components. *Composite Structures*, 2015, 132, S. 350-358. DOI 10.1016/j.compstruct.2015.05.047.
- [3] Kärger, L. Galkin, S. Zimmerling, C. Dörr, D. Linden, J. Oeckerath, A. Wolf, K. Forming optimisation embedded in a CAE chain to assess and enhance the structural performance of composite components. *Composite Structures*, 2018, 192, S. 143-152. DOI 10.1016/j.compstruct.2018.02.041.
- [4] Kunze, E. Schwarz, B. Weber, T. Müller, M. Böhm, R. Gude, M. Forming Analysis of Internal Plies of Multi-Layer Unidirectional Textile Preforms using Projectional Radiography. *Procedia Manufacturing*, 2020, 47, S. 17-23. DOI 10.1016/j.promfg.2020.04.110.
- [5] Mallach, A. Härtel, F. Heieck, F. Fuhr, JP. Middendorf, P. Gude, M. Experimental comparison of a macroscopic draping simulation for dry non-crimp fabric preforming on a complex geometry by means of optical measurement. *Journal of Composite Materials*, 2017, 51(16), S. 2363-2375. DOI: 10.1177/0021998316670477.
- [6] Khan, MA. Mabrouki, T. Vidal-Sallé, E. Boisse, P. Numerical and experimental analyses of woven composite

reinforcement forming using a hypoelastic behaviour. Application to the double dome benchmark. *Journal of Materials Processing Technology*, 2010, 210(2), S :378-388. DOI 10.1016/j.jmatprotec.2009.09.027.

[7] Machado, M. Fischlschweiger, M. Major, Z. A rate-dependent nonorthogonal constitutive model for describing shear behaviour of woven reinforced thermoplastic composites. *Composites Part A*, 2016, 80, S. 194-203. DOI 10.1016/j.compositesa.2015.10.028.

[8] Lin, H. Long, AC. Sherburn, M. Clifford, MJ. Modelling of mechanical behaviour for woven fabrics under combined loading. *International Journal of Material Forming*, 2008, 1(1), S. 899-902. DOI 10.1007/s12289-008-0241-7.

[9] Lomov, SV. Ivanov, D. Verpoest, I. Zako, M. Kurashi, T. Nakai, H. Hirosawa, S. Meso-FE modelling of textile composites: Road map, data flow and algorithms. *Composites Science and Technology*, 2007, 67(9), S. 1870–1891. DOI 10.1016/j.compscitech.2006.10.017.

[10] Sirtautas, J. Pickett, AK. Lépicier, P. A mesoscopic model for coupled drape-infusion simulation of biaxial non-crimp fabric. *Composites Part B*, 2013, 47, S. 48-57. DOI 10.1016/j.compositesb.2012.09.088.

[11] Schirmaier, F.J. Dörr, D. Henning, F. Kärger, L. A macroscopic approach to simulate the forming behaviour of stitched unidirectional non-crimp fabrics. *Composites Part A*, 2017, 102, S. 322-335. DOI 10.1016/j.compositesa.2017.08.009.

[12] Böhler, P. Härtel, F. Middendorf, P. Identification of Forming Limits for Unidirectional Carbon Textiles in Reality and Mesoscopic Simulation. *Key Engineering Materials* 2013, 554-557, S. 423-432. DOI 10.4028/www.scientific.net/KEM.554-557.423.

[13] Senner, T. Kreissl, S. Merklein, M. Meinhardt, J. Lipp, A. A modular modeling approach for describing the in-plane forming behavior of unidirectional non-crimp-fabrics. *Production Engineering Res. Devel.*, 2014, 8(5), S. 635–643. DOI: 10.1007/s11740-014-0561-z.

[14] Senner, T. Kreissl, S. Merklein, M. Meinhardt, M. Lipp, A. Bending of unidirectional non-crimp-fabrics: experimental characterization, constitutive modeling and application in finite element simulation. *Production Engineering Res. Devel.*, 2015, 9, S. 1-10. DOI: 10.1007/s11740-014-0568-5.

[15] Kärger, L. Galkin, S. Dörr, D. Poppe, C. Capabilities of Macroscopic Forming Simulation for Large-Scale Forming Processes of Dry and Impregnated Textiles. *Procedia Manufacturing*, 2020, 47, S. 140-147. DOI /10.1016/j.promfg.2020.04.155.

[16] Schirmaier, F.J. Weidenmann, K.A. Kärger, L. Henning, F. Characterisation of the draping behaviour of unidirectional non-crimp fabrics (UD-NCF). *Composites Part A*, 2016, 80, S. 28–38. DOI 10.1016/j.compositesa.2015.10.004.

[17] Galkin, J. Kunze, E. Kärger, L. Böhm, R. Gude, M. Experimental and numerical determination of the local fiber volume content of unidirectional non-crimp fabrics with forming effects. *Journal of Composites Science*, 2019, 3, 19. DOI 10.3390/jcs3010019.

[18] Dörr, D. Schirmaier, F. Henning, F. Kärger, L. A viscoelastic approach for modeling bending behavior in FE forming simulation of continuously fiber reinforced composites. *Composites Part A*, 2017, 94, S. 113-123. DOI 10.1016/j.compositesa.2016.11.027.

[19] Wolf, K. Bayrasy, P. Brodbeck, C. Kalmykov, I. Oeckerath, A. Wirth, N. MpCCI: Neutral Interfaces for Multiphysics Simulations. In: Griebel M. Schüller A. Schweitzer M (eds): *Scientific Computing and Algorithms in Industrial Simulations*. Cham: Springer International Publishing, 2017, S. 135-51. DOI: 10.1007/978-3-319-62458-7\_7.

[20] Barbagallo G. Madeo A. Azehaf I. Giorgio I. Morestin F. Boisse P. Bias extension test on an unbalanced woven composite reinforcement: Experiments and modeling via a second-gradient continuum approach. *Journal of Composite Materials* 51(2):153–170, 2017. DOI 10.1177/0021998316643577.

PDF automatically generated on 2021-05-19 11:52:56

Article url: <https://popups.uliege.be/esaform21/index.php?id=355>

published by ULiège Library in Open Access under the terms and conditions of the CC-BY License

(<https://creativecommons.org/licenses/by/4.0>)